Available online at www.sciencedirect.com
ScienceDirect
Journal of the European Ceramic Society 27 (2007) 3915–3918
www.elsevier.com/locate/jeurceramsoc

Phase evolution of $Zn_{1-x}Mn_xO$ system synthesized via oxalate precursors

M. Peiteado [a,*], A.C. Caballero [b], D. Makovec [a]

[a] *Advanced Materials Department, Jozef Stefan Institute, Jamova 39, 1000 Ljubljana, Slovenia*
[b] *Department of Electroceramics, Instituto de Cerámica y Vidrio, CSIC, 28049 Madrid, Spain*

Available online 9 March 2007

Abstract

Polycrystalline samples with nominal composition $Zn_{1-x}Mn_xO$ have been prepared by a co-precipitation technique in which kinetics of high temperature reactions are favoured by the use of highly reactive particles. Structural and compositional analysis reveal that following the decomposition of the oxalate precursor a secondary $ZnMnO_3$ phase is formed already at 400 °C. By means of XRD and HRTEM, a defect spinel-type structure is presumed for this Zn–Mn–O compound. A diluted magnetic semiconductor in which Mn atoms are homogeneously substituting Zn atoms in the semiconductor matrix is not obtained in the whole temperature range by this synthesis method. The microstructural situation is then far from that theoretically predicted for spintronic systems.

Keywords: ZnO; Dilute magnetic semiconductors; Microstructure-final

1. Introduction

Materials for spintronics (spin-based electronics) combine the complementary properties of ferromagnetic material systems and semiconductor structures. In the so called *diluted magnetic semiconductors* (DMS) a stoichiometric fraction of the host semiconductor atoms is randomly replaced by magnetic atoms and the resulting solid solution is semiconducting, but can possess well-defined magnetic properties (e.g., paramagnetic, antiferromagnetic and ferromagnetic) that conventional semiconductors do not have.[1] One of the systems which attracted more attention is that of ZnO doped with Mn, mainly because zinc oxide is a direct wide band gap semiconductor with potential utility in UV photonics and transparent electronics. A number of experimental works have been conducted reporting the appearance of ferromagnetism above 25 °C in the $Zn_{1-x}Mn_xO$ system, but in most cases the achieved results and explanations are contradictory.[2–4] The origin of such discrepancies should be found on the fact that the mechanism leading to ferromagnetic ordering is still far from understood, and this finally falls on the absence of an accurate description of the microstructure in the Zn–Mn–O system. On one hand the ionic radius of Mn^{2+} (0.66 Å) is relatively close to that for Zn^{2+} (0.60 Å), which will suggest moderate solid solubility without phase segregation. The practice shows however that magnetic ions typically exhibit low solubilities in their respective host semiconductors, i.e., the major difficulty in making ZnO ferromagnetic is the low solubility limits for magnetic impurities such as Mn^{2+} (more even at the low temperatures employed to grow the DMS material).[5] Hence the possibility that secondary-phase formation is involved should be also considered. Some approaches on the other hand suggest that the magnetic atoms form small clusters (a few atoms) producing the observed ferromagnetism in the Mn–Zn–O system,[6] and more recently it has been associated with the coexistence of Mn^{3+} and Mn^{4+} oxidation states at the diffusion front of zinc into manganese oxide.[7] Within this background the issues of structure, composition and secondary-phase formation should be carefully addressed previous to assign the origin of ferromagnetism in these transition metal-doped semiconductors. The present contribution deals with the phase evolution of the $Zn_{1-x}Mn_xO$ system in an attempt to clarify whether the real situation is so far from the theoretical predictions, in which a homogenous Mn–ZnO solid solution should be expected.

2. Experimental procedure

Magnetism in ZnO particles with small additions of Mn is very sensitive to the synthesis conditions so a single-source precursor where both ions are already intimately mixed is certainly desirable. Polycrystalline samples with nominal

* Corresponding author. Tel.: +386 1 4773629; fax: +386 1 4773875.
E-mail address: marco.peiteado@ijs.si (M. Peiteado).

0955-2219/$ – see front matter © 2007 Elsevier Ltd. All rights reserved.
doi:10.1016/j.jeurceramsoc.2007.02.062

composition $Zn_{1-x}Mn_xO$ ($x = 0$, 0.01, 0.02, 0.05, 0.1 and 0.2) were thus prepared via an oxalate precursor, which in addition decomposes in clean manner to give metal oxides. The oxalate precursor $Zn_{1-x}Mn_x(C_2O_4)\cdot 2H_2O$ was obtained by room temperature co-precipitation of aqueous solutions of zinc and manganese acetates, $Zn(CH_3COO)_2\cdot 2H_2O$ and $Mn(CH_3COO)_2\cdot 4H_2O$, with oxalic acid. More details on the synthesis method are described elsewhere.[8]

Thermal evolution of the samples was followed by differential thermal analysis and thermogravimetry (DTA-TG) on a Netzsch STA 449 C instrument in air atmosphere at a heating rate of 5 °C/min. In order to understand the nature of the involved phases, samples were calcined at different temperatures ranging from 400 to 1000 °C for 12 h. Grounded powders were then characterized by X-ray diffraction (XRD) using a Bruker AXS Endaevor 4 Diffractometer. For TEM investigations the calcined powders were deposited on a copper-grid-supported transparent carbon foil. The samples were examined by a field-emission electron-source high resolution transmission electron microscope HRTEM (JEOL 2010 F), operated at 200 kV. The microscope is equipped with an EDS microanalysis system (LINK ISIS EDS 300).

3. Results and discussion

Given the level of dilution of the magnetic atoms in the ZnO compositions with lower additions of Mn, the evolution of the system is more easily followed on the composition with the higher amount of dopant, that is $x = 0.2$, although a similar behaviour was obtained for all other compositions. Fig. 1 depicts DTA-TG curves of sample $Zn_{0.8}Mn_{0.2}O$ and shows the thermal decomposition of the oxalate precursor: an endothermic dehydration of the oxalate around 160 °C and its exothermic decomposition below 400 °C, with a total weight loss (WL) of 56.5%. Above this temperature no significant changes were detected in the curves, particularly in TG, although they could be masked by the total weight loss of the oxalate. To verify this feature the same composition was calcined at 400 °C for 48 h (oxalate decomposition completed) and DTA-TG analyses were repeated. A small and continuous weight loss was observed during the whole heating range, but again with no sharp changes in the DTA curve. However, thermochemistry of manganese oxides in air atmosphere is known to involve different redox reactions above 500 °C,[9] which are not being detected here. So apparently

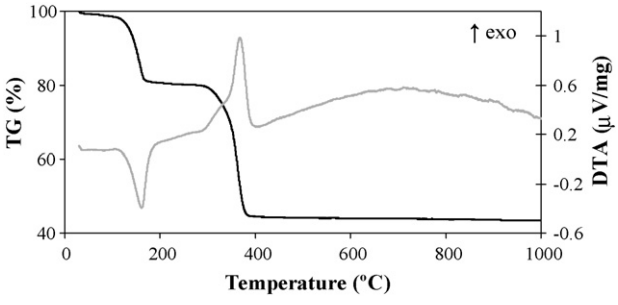

Fig. 1. TG/DTA curves of the oxalate precursor for sample with nominal composition $Zn_{0.8}Mn_{0.2}O$.

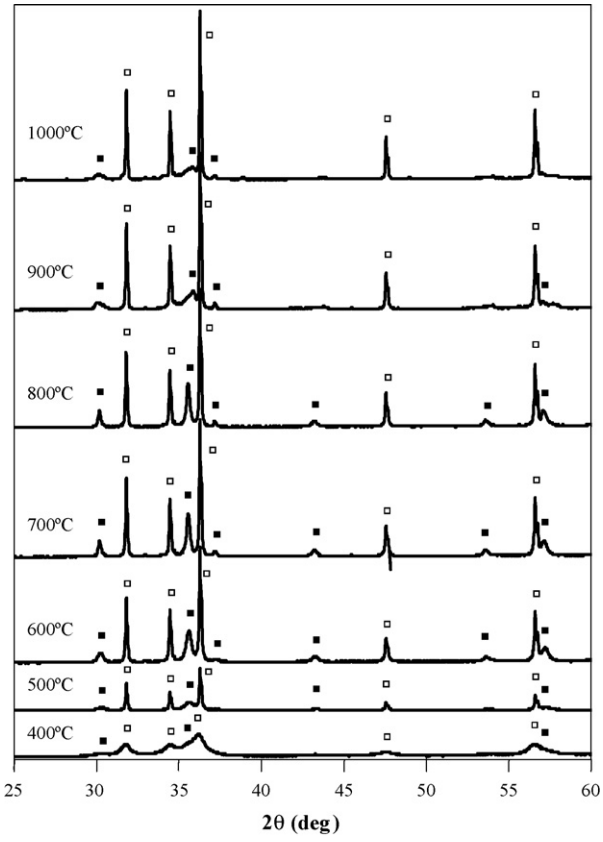

Fig. 2. XRD patterns of $Zn_{0.8}Mn_{0.2}O$ powder samples calcined for 12 h at different temperatures (□, ZnO; ■, $ZnMnO_3$).

the kinetics of the different processes involving changes in the oxidation state of manganese is being altered by the presence of zinc oxide.

Fig. 2 shows the XRD patterns of $Zn_{0.8}Mn_{0.2}O$ powder samples treated at different calcination temperatures. As observed, already after calcination for 12 h at 400 °C (that is above the decomposition temperature of the oxalate precursor), broad peaks of diffraction are obtained that suggest partial crystallinity. With temperature these peaks become sharper due to crystallite growth, and then it is possible to see that besides the large peaks corresponding to the ZnO wurtzite structure, smaller peaks of a secondary phase are also present. These peaks match to the pattern of $ZnMnO_3$ compound which crystallizes on a cubic symmetry with lattice parameter $a = 8.35$ Å (JCPDF file no. 19–1461). This last compound has been previously detected by other authors,[3,10,11] although not at such low temperatures. Moreover, its structure has not been reported jet. However, from the similarity of its XRD pattern with the pattern of spinel it could be concluded that it has spinel-related structure. Increasing the temperature leads to an increase in the total amount of this secondary phase, which reaches a maximum around 800 °C; in fact at this temperature it can be detected even in the systems with lower additions of manganese (see Fig. 3). At calcination temperatures above 800 °C, the intensity of these secondary-phase peaks decreases, they become broader and their position is shifted. Most probably, the compound $ZnMnO_3$ decomposes above ~800 °C and one or more new compounds are formed.

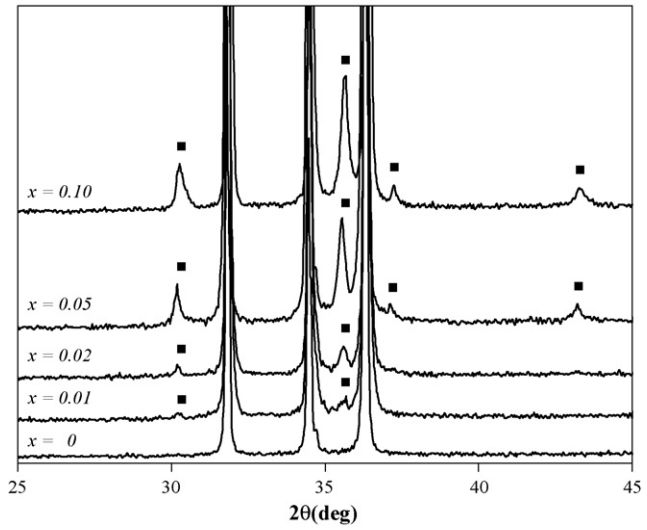

Fig. 3. XRD powder patterns of samples with different $Zn_{1-x}Mn_xO$ nominal composition, after calcination for 12 h at 800 °C (■, $ZnMnO_3$; rest of the peaks belonging to ZnO phase).

Identification of these compounds with XRD is hampered by the overlapping and low intensity of the different peaks.

Fig. 4a shows TEM image of composition $Zn_{0.8}Mn_{0.2}O$ after calcining at 500 °C. Two types of particles can be observed: particles in shape of hexagonal prisms of approximately 300 nm in size, and smaller particles with an average size of ~15 nm (see inset in Fig. 4a) arranged together in the form of large platelet-like agglomerates. Selected area electron diffraction (SAED) pattern taken from the larger particles (Fig. 4b) match with the ZnO wurtzite structure. Also EDS analyses of these particles evidence the presence of just zinc and oxygen, without any trace of manganese. On the other hand, SAED pattern taken from the agglomerate of smaller particles (Fig. 4c) shows diffraction rings characteristic of a polycrystalline sample that can be indexed according to a spinel structure. EDS of individual particle of these agglomerates indicate both the presence of zinc and manganese. Quantification of the spectra yields a Zn/Mn ratio close to 1, so matching the $ZnMnO_3$ formula.

The general appearance of the two-phase system does not change much with temperature as followed by TEM, apart from increase in particles size. ZnO particles had size of 12 nm after calcination at 400 °C and grow up to 900 nm at 800 °C. The particles of the secondary phase grow from 7 nm at 400 °C to 50 nm at 800 °C however they remain agglomerated in these plate-like agglomerates. The origin of the agglomerate shape should be attributed to the precursor employed. Above 800 °C these agglomerates start to react and disappear, which is consistent with the results obtained with XRD.

According to these results it is inferred that when preparing samples with nominal composition $Zn_{1-x}Mn_xO$ by a method that provides good homogeneity, a binary system is obtained comprising ZnO and a secondary $ZnMnO_3$ phase. This last one, which points towards a spinel-like structure, is formed simultaneously with the decomposition of the oxalate precursor at temperatures as low as 400 °C and remains stable till 800 °C. The confinement of manganese into the $ZnMnO_3$ structure slows down the kinetics of the different reduction processes of manganese. This comes to explain the absence of significant signals in the DTA-TG curves above 400 °C. On the other hand, the presence of manganese in this secondary phase also seems to reduce the possibility of Mn–ZnO solid solution at low temperatures. At higher temperatures we could not clarify what is happening with the Mn after the $ZnMnO_3$ decomposition, but again a homogeneous diluted magnetic semiconductor is not found. In other words a homogeneous sample with Mn atoms

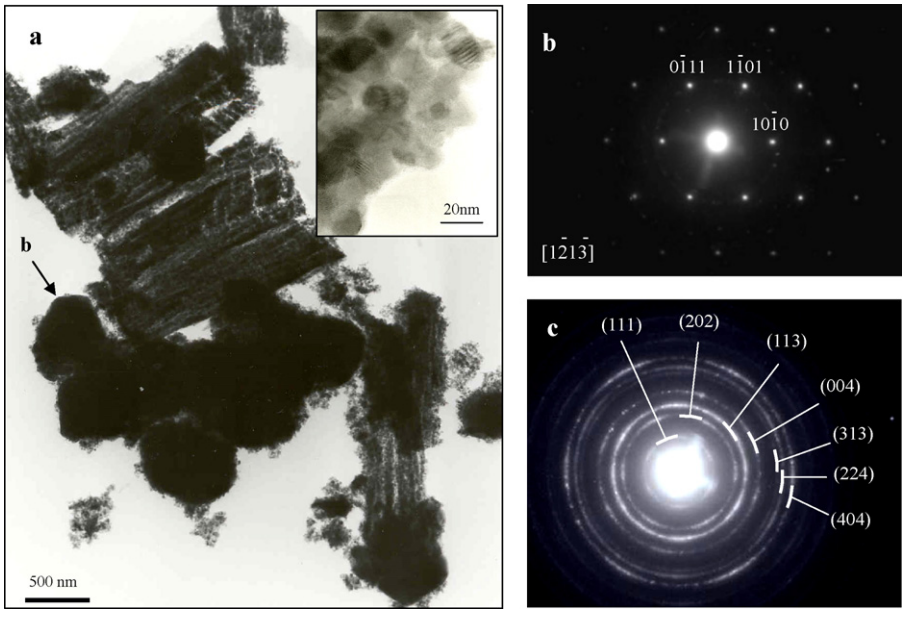

Fig. 4. Microstructure of $Zn_{0.8}Mn_{0.2}O$ sample calcined for 12 h at 500 °C. (a) Bright field TEM image. Inset shows magnified part of the agglomerates of small particles of secondary phase. (b) SAED pattern taken from the large particle marked in the micrograph with b. The pattern was indexed according to the ZnO wurtzite structure along the [1-21-3] direction. (c) SAED pattern taken from the agglomerates of small particles, indexed according to a spinel related structure (cubic, $a = 0.835$ nm).

substituting Zn atoms of the ZnO matrix is never obtained by this reactive method. Hence and, although no magnetic characterization is reported in this paper, the fact is that even if these samples show ferromagnetic behaviour, the microstructural situation is really far from that predicted theoretically and new mechanisms should be addressed to describe the ferromagnetic response in this system.[7] Nevertheless further experiments are in progress to more precisely determine the magnetic behaviour, the structure and the thermal evolution of this co-precipitated system as well as of the pure $ZnMnO_3$ phase.

4. Conclusions

The phase evolution of ZnO ceramics with small additions of Mn was studied on a highly reactive co-precipitated system. Following the decomposition of the oxalate precursor, the formation of a $ZnMnO_3$ secondary phase is observed at temperatures as low as 400 °C. A defect spinel-type structure with manganese probably in different oxidation states is presumed for this Zn–Mn–O phase. Although the decomposition of this phase at high temperature remains to be described, a diluted magnetic semiconductor in which Mn atoms are homogeneously substituting Zn atoms in the semiconductor matrix is not obtained by this method in the whole temperature range.

Acknowledgments

The authors would like to express their gratitude to the Ministry of Higher Education, Science and Technology of Slovenia for the financial support. Dr. Peiteado also acknowledges the Secretaría de Estado de Universidades e Investigación del Ministerio de Educación y Ciencia (Spain). This work has been conducted within CICYT MAT 2004-04843-C02-01 project.

References

1. Dietl, T., Ohno, H., Matsukura, F., Cibert, J. and Ferrand, D., Zener model description of ferromagnetism in zinc-blende magnetic semiconductors. *Science*, 2000, **287**(5455), 1019–1022.
2. Sharma, P., Gupta, A., Rao, K. V., Owens, F. J., Sharma, R., Ahuja, R. *et al.*, Ferromagnetism above room temperature in bulk and transparent thin films of Mn-doped ZnO. *Nat Mater*, 2003, **2**(10), 673–677.
3. Kundaliya, D. C., Ogale, S. B., Lofland, S. E., Dhar, S., Meeting, C. J., Shinde, S. R. *et al.*, On the origin of high-temperature ferromagnetism in the low-temperature processed Mn–Zn–O system. *Nat Mater*, 2004, **3**(10), 709–714.
4. Costa-Krämer, J. L., Briones, F., Fernández, J. F., Caballero, A. C., Villegas, M., Díaz, M. *et al.*, Nanostructure and magnetic properties of the ZnMnO system, a room temperature magnetic semiconductor? *Nanotechnology*, 2005, **16**(2), 214–218.
5. Chambers, S. A. and Yoo, Y. K., New materials for spintronics. *Mater Res Bull*, 2003, **28**(10), 706–708.
6. Van Schilfgaarde, M. and Mryasov, O. N., Anomalous exchange interactions in III–V dilute magnetic semiconductors. *Phys Rev B*, 2001, **63**(23), 233205.
7. García, M. A., Ruíz-González, M. L., Quesada, A., Costa-Krämer, J. L., Fernández, J. F., Khatib, S. J. *et al.*, Interface double-exchange ferromagnetism in the Mn–Zn–O system: new class of biphase magnetism. *Phys Rev Lett*, 2005, **94**(21), 217206.
8. Bouloudenine, M., Viart, N., Colis, S., Kortus, J. and Dinia, A., Antiferromagnetism in bulk $Zn_{1-x}Co_xO$ magnetic semiconductors prepared by the co-precipitation technique. *Appl Phys Lett*, 2005, **87**(5), 052501.
9. Zaki, M. I., Hasan, M. A., Pasupulety, L. and Kumari, K., Thermochemistry of manganese oxides in reactive gas atmospheres: probing redox compositions in the decomposition course $MnO_2 \rightarrow MnO$. *Termochim Acta*, 1997, **303**(2), 171–181.
10. Thota, S., Dutta, T. and Kumar, J., On the sol–gel synthesis and thermal, structural, and magnetic studies of transition metal (Ni, Co, Mn) containing ZnO powders. *J Phys: Condens Mater*, 2006, **18**(8), 2473–2486.
11. Cong, C. J., Liao, L., Liu, Q. Y., Li, J. C. and Zhang, K. L., Effects of temperature on the ferromagnetism of Mn-doped ZnO nanoparticles and Mn-related Raman vibration. *Nanotechnology*, 2006, **17**(5), 1520–1526.